NURETH14-265

COUPLED DNS/RANS SIMULATION OF FISSION GAS DISCHARGE DURING LOSS-OF-FLOW ACCIDENT IN GEN-IV SODIUM FAST REACTOR

I.A. Bolotnov¹, F. Behafarid², D. Shaver², S.P. Antal², K.E. Jansen³ and M.Z. Podowski²

North Carolina State University, Raleigh, North Carolina, USA
Center for Multiphase Research, Rensselaer Polytechnic Institute, Troy, New York, USA
University of Colorado, Boulder, Colorado, USA

Abstract

The objective of this paper is to give an overview of a multiscale modeling approach to three-dimensional two-phase transient computer simulations of the injection of a jet of gaseous fission products into a partially blocked SFR coolant channel following localized cladding overheat and breach. The phenomena governing accident progression have been resolved at two different spatial and temporal scales by the inter-communicating computational multiphase fluid dynamics codes: PHASTA (at DNS level) and NPHASE-CMFD (at RANS level). The issues discussed in the paper include an overview of the proposed three dimensional (3D) two-phase flow models of the inter-related phenomena which occur as a result of cladding failure and the subsequent injection of a jet of gaseous fission products into partially blocked SFR coolant channels and gas/molten sodium transport along the channels. An analysis is presented on the consistency and accuracy of the models used in the simulations, and the results are shown of the predictions of gas discharge and gas/liquid-metal two-phase flow in a multichannel fuel assembly. Also, a discussion is given of the major novel aspects of the overall work.

1 Introduction

The technological and safety standards set for future Generation IV (Gen-IV) Reactors can only be achieved if advanced simulation capabilities become available, which combine high performance computing with the necessary level of modeling detail and high accuracy of predictions. Given the limitations of current generation of supercomputers, a practical approach which would be capable of satisfying the combined goals of accuracy and computational efficiency is based on the use of computational models of different scales. The most important and challenging aspect of such an approach is associated with the development of interfaces which will allow for a direct interactive coupling between the individual models and the corresponding numerical solvers (or computer codes).

The purpose of this paper is to present a multiscale modeling approach to computer simulations of the progression of an accident in the proposed Gen. IV Sodium fast Reactor (SFR). In the assumed scenario, the accident is caused by a partial blockage of a coolant channels at the inlet to the hot fuel assembly. As a consequence, the hottest fuel element becomes overheated and experiences a localized cladding failure. This, in turn, causes a release of hot fission products into the surrounding coolant channels and gas/molten-sodium flow toward the exit of the core. Schematic of the consequences of local cladding failure is shown in Figure 1. The analysis has been performed at two different spatial and temporal

scales using the inter-communicating computer codes: PHASTA (at DNS level) and NPHASE-CMFD (at RANS level).

Modeling of the fission gas escape using a direct numerical simulation (DNS) approach is highly desirable because the models characteristic of the Reynolds averaged Navier-Stokes (RANS) method may not be applicable to the complex phenomena involved. However, downstream of the cladding failure zone, the flow characteristics are much better suited to a RANS approach.

Since the initial results of the work on this multiyear project were reported before (Bolotnov et al., 2010b), the focus of this paper is on the recent modeling advancements, such as the modeling of time-dependent fission gas discharge from the failed fuel rod, pressure feedback in the two-code coupling, and the effect of liquid sodium turbulence.

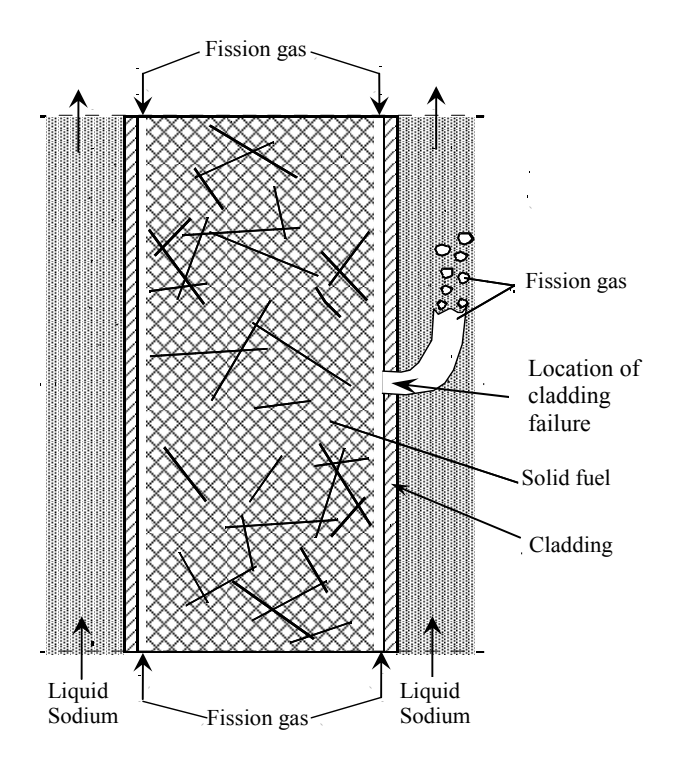


Figure 1. Schematic of fission gas escape following cladding failure in SFR.

2 Description of Computer Codes

A brief description of the major features of the PHASTA and NPHASE-CMFD codes is presented in this section. Also, several references are given to the previous studies which document the results of extensive testing and validation of the individual models and computational methodologies used in both codes.

2.1 The PHASTA code

PHASTA (Whiting and Jansen, 2001; Jansen et al., 2000) is a parallel, hierarchic (between 2nd- and 5th orders of accuracy, depending on function choice), adaptive, stabilized (finite element) transient analysis DNS flow solver (both incompressible and compressible). PHASTA was the first unstructured grid LES code, and it has been applied to turbulent flows ranging from validation benchmarks (channel flow, decay of isotropic turbulence) to complex flows (airfoils at maximum lift, flow over a cavity, near lip jet engine flows and fin-tube heat

exchangers). The PHASTA code uses advanced anisotropic adaptive algorithms (Sahni et al., 2006) and the most advanced LES/DES models (Tejada-Martinez and Jansen, 2005). The two-phase version of PHASTA utilizes the Level Set method to define the interface between the gas and liquid phases (Sethian, 1999). The combined DNS/Level-Set model has been extensively tested and validated for various two-phase flow problems and conditions, including a study on bubble dynamics (Nagrath et al., 2005) and the effect of turbulence on bubble shape and distribution (Bolotnov et al., 2011).

2.2 NPHASE-CMFD

NPHASE-CMFD (Antal et al., 2000) is an advanced Computational Multiphase Fluid Dynamics computer code for the simulation and prediction of combined mass, momentum and energy transfer processes in a variety of single-phase (Gallaway et al., 2008) and multiphase/multiscale systems, including gas/liquid (Wierzbicki et al., 2007; Tselishcheva et al., 2010), solid/liquid (Tiwari et al., 2006; 2009) and gas/solid/liquid (Antal et al., 2000) flows. It uses two-phase k-ɛ models of turbulence (the user can chose between the high Reynolds number and low Reynolds number options of the model). The mixture and field continuity equations can be solved in a coupled or segregated (uncoupled) manner, using stationary coefficient linearization. The code is fully unstructured and can utilize second-order accurate convection and diffusion discretization. The technology used by the NPHASE-CMFD code is an ensemble averaged multifield model of two-phase or multiphase flows.

3 Model Description

3.1 Problem Formulation

As mentioned before, the purpose of the present work was to develop and implement a multiscale three dimensional (3D) modeling approach to the inter-related phenomena which occur as a result of fuel element heatup and cladding failure, including the injection of a jet of gaseous fission products into a partially blocked SFR coolant channel, and gas/molten sodium transport along the coolant channels.

The overall model included the following phenomena:

- pressurized fission gas escape from the fuel rod into the liquid sodium coolant,
- two-phase side jet injection into the coolant channels,
- transient two-phase flow propagation downstream of the location of cladding failure.

Direct numerical simulations of two-phase turbulent flow have been performed by the PHASTA code with a built-in Level Set algorithm. The model allows one to track the evolution of gas/liquid interfaces at a millimeter scale. The simulated phenomena include the formation and breakup of the jet of fission products injected into the turbulent liquid sodium coolant. The transient gas injection rate has been computed by PHASTA based on local pressure fluctuations at the cladding failure, the initial pressure inside the fuel rod and the assumed flow resistance between the fuel and the stainless steel cladding.

To convert the PHASTA results into a format compatible with the RANS code, NPHASE-CMFD, the fluctuating turbulent two-phase virtual data has been averaged at different locations over time to obtain mean phasic velocities and volumetric concentrations, as well as the liquid turbulent kinetic energy and turbulence dissipation rate. A sliding window time-average has been used to capture mean flow parameters for transient cases.

Using the input provided by PHASTA, fuel-assembly scale (compatible with core height) simulations of turbulent liquid-sodium/fission-gas mixture flow in reactor coolant channels have been performed by the NPHASE-CMFD code. The coupled use of these two codes made it possible to perform full scale simulations of hypothetical accidents in future Gen-IV reactors, while maintaining the required level of detail at different modeling scales.

To assure the numerical consistency and physical accuracy of the results of predictions, thorough test studies were performed for both PHASTA and NPHASE-CMFD (Bolotnov et al, 2009, 2010a, 2010b) on issues such as the effect of computational grids, code convergence and others.

3.2 Computational Domains

Figure 2 shows the physical domains used by both PHASTA and NPHASE-CMFD. The large scale simulation performed using the NPHASE-CMFD code is capable of resolving the entire fuel rod assembly (only a small fraction of this domain is shown in Figure 2). This is done using a RANS approach and by tracking the gas volume fraction and averaged turbulent flow parameters. To accurately predict fission gas escape through the damaged fuel rod cladding, a DNS approach has been applied within 10 mm of the cladding failure location using the PHASTA code. The unstructured mesh capabilities of both PHASTA and NPHASE-CMFD allow for efficient modeling of the jet propagation in the complex flow domain between the fuel rods.

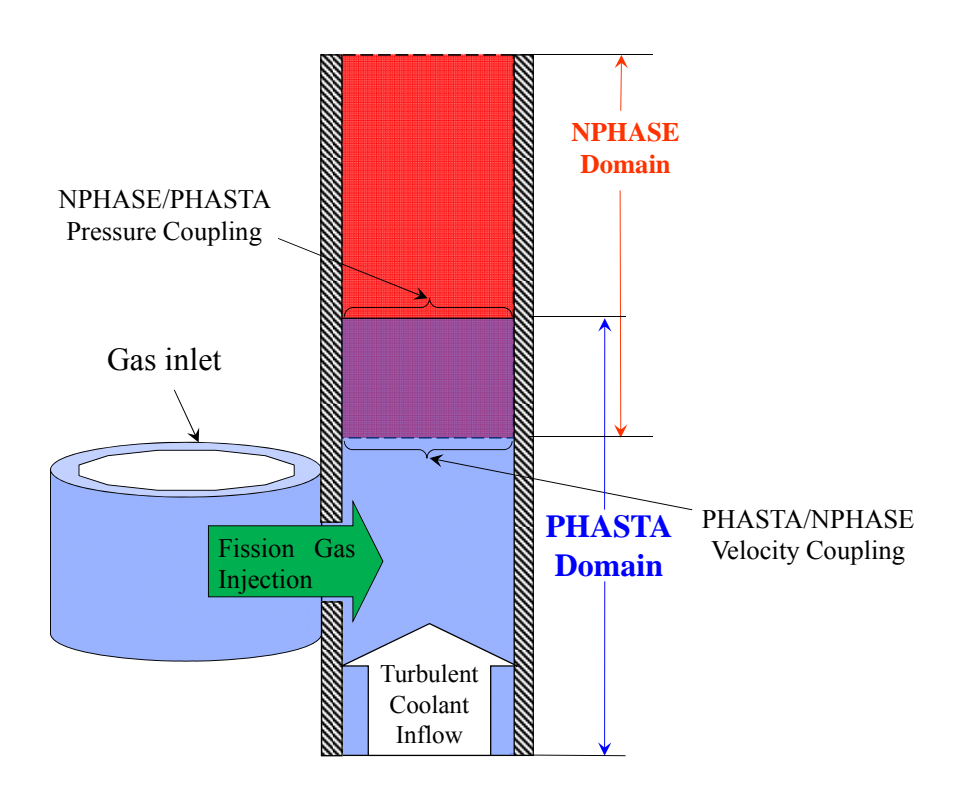


Figure 2. Overview of computational domains.

3.2.1. NPHASE-CMFD computational domain

The computational domain of NPHASE, a cross-section of which is shown in Figure 3, actually encompasses and extends along the coolant channels around 30 fuel rods. The mesh used in the NPHASE simulation is axially non-uniform and consists of approximately 1.1 million elements. Since the NPHASE mesh is much coarser than the PHASTA mesh, data is interpolated from the PHASTA mesh onto the NPHASE mesh to generate the inlet conditions for the NPHASE simulation. The total physical length of the NPHASE domain is 0.5m. This, in turn, illustrates the advantages of coupling the DNS results of PHASTA, limited for practical reasons to a relatively small computational domain, with the NPHASE-based large-scale model which uses accurate PHASTA predictions as input (Bolotnov et al., 2009).

3.2.2. PHASTA computational domain

The PHASTA domain is about 50 mm tall and includes the region around the cladding failure zone as well as a section of the coolant channel which starts below the breach and extends to a short distance above the breach. This is shown in Figure 4. To set up the gas inflow boundary conditions in PHASTA, the gas flow rate is computed analytically as a function of the pressure difference between the top of the cladding and the cladding failure zone using the porous media model for the gas flow through the gap between the fuel rod and the cladding. Other boundary conditions are: a no-slip condition applied on all solid surfaces, and a pressure boundary condition that corrects for the effects of surface tension at the outflow of the domain. This outflow pressure is supplied by the NPHASE flow solver.

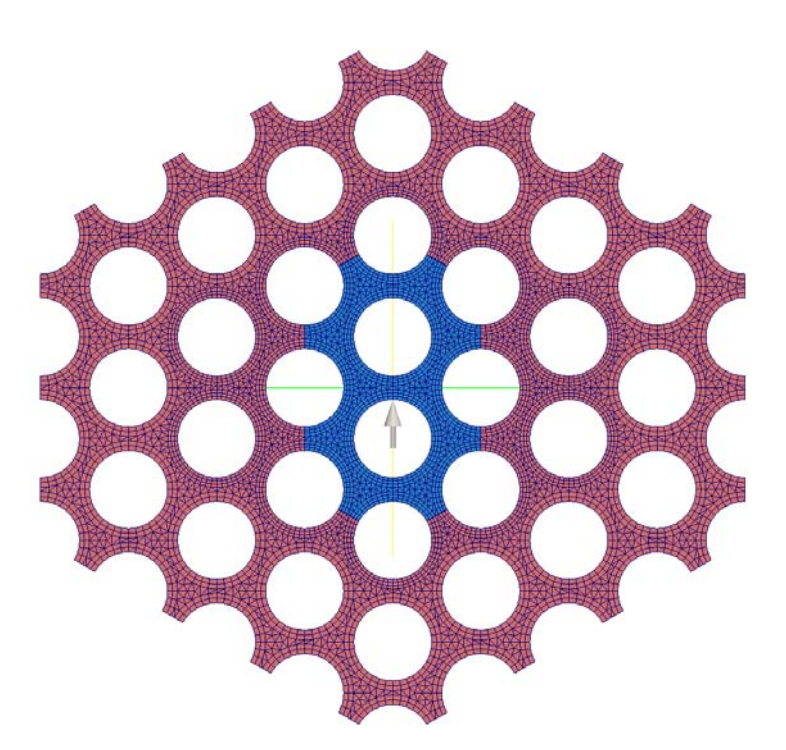


Figure 3. NPHASE-CMFD domain: Cross section of the NPHASE domain showing overlap with the PHASTA domain (blue) and the added coolant channels (red), the arrow indicates the location of gas jet injection.

The 14th International Topical Meeting on Nuclear Reactor Thermalhydraulics, NURETH-14 Toronto, Ontario, Canada, September 25-30, 2011

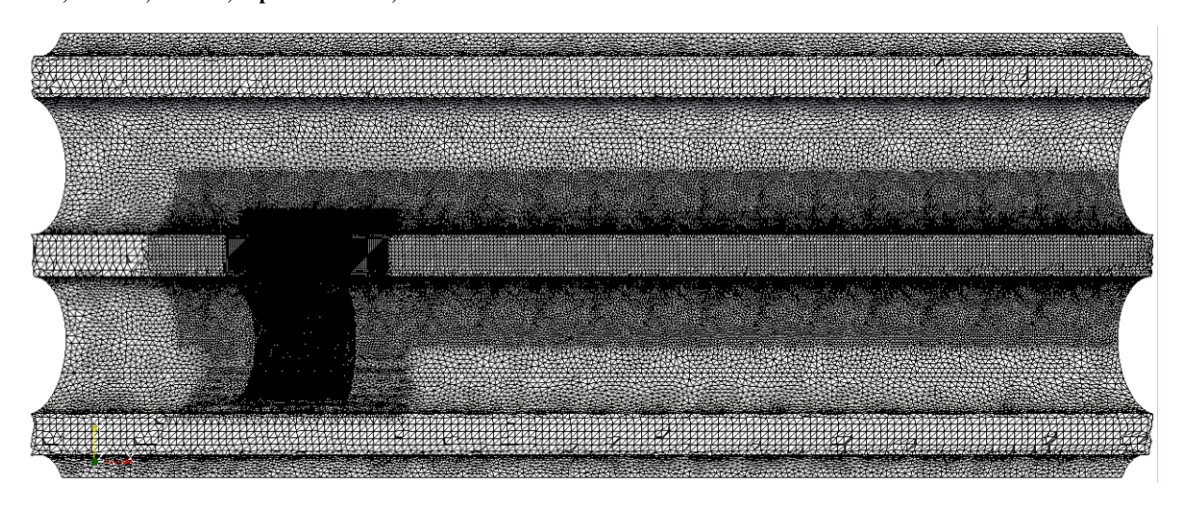


Figure 4. Computational mesh used in the PHASTA simulations for laminar coolant flows.

3.3 Description of mathematical models

3.3.1 PHASTA models

Whiting and Jansen (2001) provided a detailed description of the finite element formulation used in the PHASTA code. The strong form of the INS equations is given by

Mass conservation

$$u_{i,j} = 0 \tag{1}$$

Momentum conservation

$$\rho u_{i,t} + \rho u_j u_{i,j} = -\hat{p}_{,i} + \hat{\tau}_{ij,j} + \hat{f}_i$$
 (2)

where ρ is density, u_i is the *i*-th component of velocity, $\hat{p}_{,i}$ is pressure, $\hat{\tau}_{ij}$ is the stress tensor, and \hat{f}_i represents body forces along the *i*-th coordinate.

For the incompressible flow of a Newtonian fluid, the stress tensor is related to the strain rate tensor, S_{ij} , as

$$\hat{\tau}_{ij} = 2\mu S_{ij} = \mu(u_{i,j} + u_{j,i}) \tag{3}$$

The level set method (Sethian, 1999) involves modeling the interface as the zero level set of a smooth function, φ , where φ represents the signed distance from the interface. Using the Continuum Surface Tension (CST) model of Brackbill et al. (1992), the surface tension force is computed as a local interfacial force density, which is included in \hat{f}_i . The described approach has been recently used by Bolotnov et al. (2011) to perform detached DNS of turbulent bubbly channel flow and statistically analyze it.

3.3.2 NPHASE modelling concept

The multiphase model in the NPHASE-CMFD code is based on the multifield modeling concept. The ensemble-averaged mass and momentum equations, respectively, are given by

The 14th International Topical Meeting on Nuclear Reactor Thermalhydraulics, NURETH-14 Toronto, Ontario, Canada, September 25-30, 2011

Mass conservation

$$\frac{\partial \left(\alpha_{k} \rho_{k}\right)}{\partial t} + \nabla \cdot \left(\alpha_{k} \rho_{k} \overline{\mathbf{v}}_{k}\right) = \Gamma_{k} \tag{4}$$

Momentum conservation

$$\frac{\partial \left(\alpha_{k} \rho_{k} \overline{\mathbf{v}}_{k}\right)}{\partial t} + \nabla \cdot \left(\alpha_{k} \rho_{k} \overline{\mathbf{v}}_{k} \right) = -\alpha_{k} \nabla \overline{p}_{k} - \sum_{j} (\overline{p}_{k} - p_{kj}^{i}) \nabla \alpha_{k} + \alpha_{k} \nabla \cdot \underline{\underline{\mathbf{\tau}}}_{k}^{i} + \sum_{j} (\underline{\underline{\mathbf{\tau}}}_{k}^{i} - \underline{\underline{\mathbf{\tau}}}_{kj}^{i}) \nabla \alpha_{k} + \sum_{j} \mathbf{M}_{kj}^{i} + \alpha_{k} \rho_{k} \mathbf{g}$$

$$(5)$$

In Eqs.(4)–(5), (j,k) are the field indices, the subscript 'i' refers to the interfacial parameters, \mathbf{M}_{kj}^{i} is the interfacial force per unit volume exerted by field-j on field-k, and the remaining notation is conventional.

3.4 Boundary conditions and interfaces between the codes

To achieve coupling between the two codes used in the analysis, a consistent data transfer must be provided between the individual codes. A file-based data transfer method has been used to transfer the multiphase inflow boundary conditions needed by the "downstream" software using additional processing, such as space and time interpolation as well as averaging techniques when converting the DNS results into RANS inflow boundary conditions. In order to fully couple the codes, a pressure feedback has been developed as a data transfer method from NPHASE-CMFD to PHASTA. Thus, PHASTA time-transient solution directly depends upon the large scale dynamics modeled by NPHASE-CMFD.

3.4.1 PHASTA to NPHASE-CMFD data transfer

As mentioned before, the DNS results produced by the PHASTA code require averaging before they can be used by NPHASE-CMFD as inflow boundary conditions. The following technique has been developed to provide the boundary conditions for the NPHASE domain:

- A list of coordinates at the NPHASE domain inflow is generated.
- At every time step of PHASTA execution instantaneous velocity components (u_1 , u_2 , u_3) and distance to interface field are interpolated from PHASTA solution at the NPHASE coordinates.
- A post-processing code performs the analysis of the data and computes the mean velocity distribution (U_1^k, U_2^k, U_3^k) , volume fraction, turbulent kinetic energy and turbulence dissipation rate, for each flow field, k (e.g., k = 1 for liquid and k = 2 for gas).

For transient flow we perform sliding window averaging. The analysis results in the following time-dependent functions of the described quantities:

$$U_k^i(t) = \frac{1}{\alpha_k N_w} \sum_{j=1}^{N_w} X_k u_m^i \left(t + t_j \right) \qquad k_k(t) = \frac{1}{\alpha_k N_w} \sum_{j=1}^{N_w} X_k \sum_{i=1}^{3} \frac{1}{2} \left(u_m^{ii}(t + t_j) \right)^2$$
 (6)

$$\varepsilon_{k}(t) = v \frac{1}{\alpha_{k} N_{w}} \sum_{j=1}^{N_{w}} \sum_{i=1}^{3} \sum_{k=1}^{3} X_{k} \frac{\partial u_{m}^{\prime i}(t+t_{j})}{\partial x_{k}} \qquad \alpha_{k}(t) = \frac{1}{N_{w}} \sum_{j=1}^{N_{w}} X_{k}(t+t_{j})$$
(7)

where X_k is the phase indicator function for field k, $u_m^{i}(t+t_j) = u_m^i(t+t_j) - U^i(t)$ is the fluctuation of velocity component i computed during the ensemble run m at the time instant $t + t_j$; N_w is the number of velocity samples in each window, t is the current time, $t_j = (j - N_w/2)\Delta t$ is the local window time, Δt is the time step.

The sliding window averaging technique is dependent on the difference in time step size between the NPHASE simulation and the PHASTA simulation. The NPHASE code uses a time step size of 0.5 ms, which is significantly larger than the time step used in the PHASTA simulation. This in turn allows for averaging of a large set of data to generate the NPHASE inflow boundary conditions using a window of 5 ms. If necessary, the width of the sliding window can be adjusted to account for the number of PHASTA time steps available as well as to capture the overall transient nature of the PHASTA simulation.

3.4.2 Pressure feedback from NPHASE-CMFD to PHASTA

The NPHASE-CMFD code provides pressure information at the interface plane between the NPHASE and PHASTA domains. This plane is located 50 mm downstream from the center of the fuel rod failure. NPHASE averages the pressure over the area encompassed by the PHASTA simulation and records this value. The information is exchanged at predetermined time intervals. PHASTA uses the average pressure computed by NPHASE as the outflow BC. This transfer of information from a large scale simulation back to a detailed DNS model allows one to account for the changing pressure conditions in the domain (e.g. due to changing average density of two-phase mixture) and the influence of these conditions on local fission gas discharge in the cladding failure zone.

4 Results of Multiscale Simulations

The models discussed in Section 3 have been used to simulate the consequences of a loss-of-flow accident in a Gen. IV Sodium fast reactor (SFR). The phenomena modeled included the injection of pressurized fission gas into the coolant channels surrounding the failed fuel element and the transport of gas/liquid-sodium mixture toward the top of the core. Typical results of the multiscale simulations are presented next.

4.1 Laminar inflow case

The PHASTA code has been used to perform the two-phase DNS of gas jet injection. A series of numerical tests have been performed to develop and test the ability of PHASTA to handle variable gas inflow profiles through growing cladding failure shapes. The results shown in Figure 5 correspond to the cladding breach area of 3 mm², the initial gas pressure of 0.6 MPa and the reactor coolant pressure of 0.3 MPa. The corresponding initial fission gas volumetric flow rate was 10.1×10^{-6} m³/s and the average inlet velocity of liquid sodium coolant was 0.08 m/s. The latter value corresponds to laminar flow conditions (consistent with the channel-blockage accident scenario).

4.1.1 PHASTA calculations

The finite element mesh used in PHASTA simulation for the laminar liquid coolant flow case is shown in Figure 4. To let PHASTA properly represent the interface, the mesh has been refined around the cladding failure zone and in the regions where the interface propagates.

The computational mesh has been designed to provide adequate resolution for interface tracking in the region of interest and has around 1.5 million nodes and 8.4 million elements. The results of the gas injection simulation are presented for three different time instants. The present two-phase PHASTA simulation was performed on 2,048 IBM BlueGene/L processors for about 500 wall clock hours, which corresponds to approximately more than 1 million CPU-hours.

The PHASTA simulation results have been averaged using a plane of virtual probes located normal to the coolant flow direction at the distance of 7 mm from the center of the fission gas inflow. The location of the data gathering plane is shown by a white gap between the computational domains in Figure 6. The averaged data was then supplied to the NPHASE-CMFD RANS-based simulation as the inflow boundary condition.

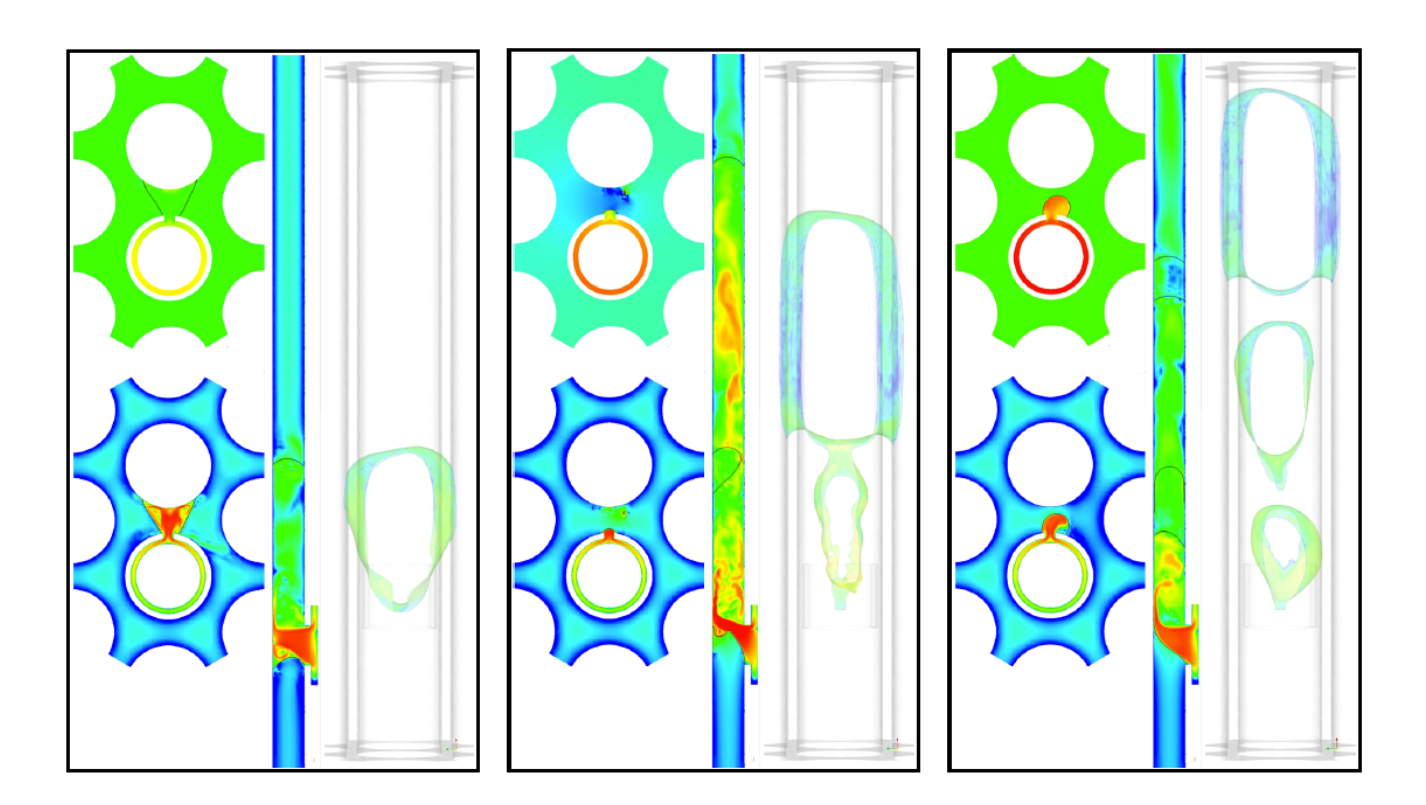


Figure 5. Laminar case PHASTA simulation results at physical times of 0.08, 0.23 and 0.33 second. Each set has two top-views of pressure and velocity fields (left), one side view of the velocity field (middle) and a 3D shape of the interface colored by velocity (right). The interface is shown as a black line.

4.1.2 NPHASE-CMFD Calculations

The NPHASE-CMFD model has been used to determine how the gas released into the coolant spreads as it travels along the coolant channel. The results of simulations are shown in Figure 9. Figures 9(a) and 9(b) present the predicted axial velocities of liquid sodium and fission gas, respectively, and Figure 7(c) illustrates how the volume fraction of gas changes along the reactor channel. The turbulent dispersion force causes the gas to spread over a significant portion of the channel cross section. The complex inlet flow pattern is a direct result of large scale eddies produced by the jet hitting the neighboring fuel rods. These are long standing fluid structures which are not eliminated by the time-averaging done on the PHASTA data. Downstream from the jet, these structures decay into a much less chaotic flow. As can be seen in Figure 7(b), the gas velocity increases along the channel due to gravity. This causes a drop in volume fraction which is observed in the initial section of the channel.

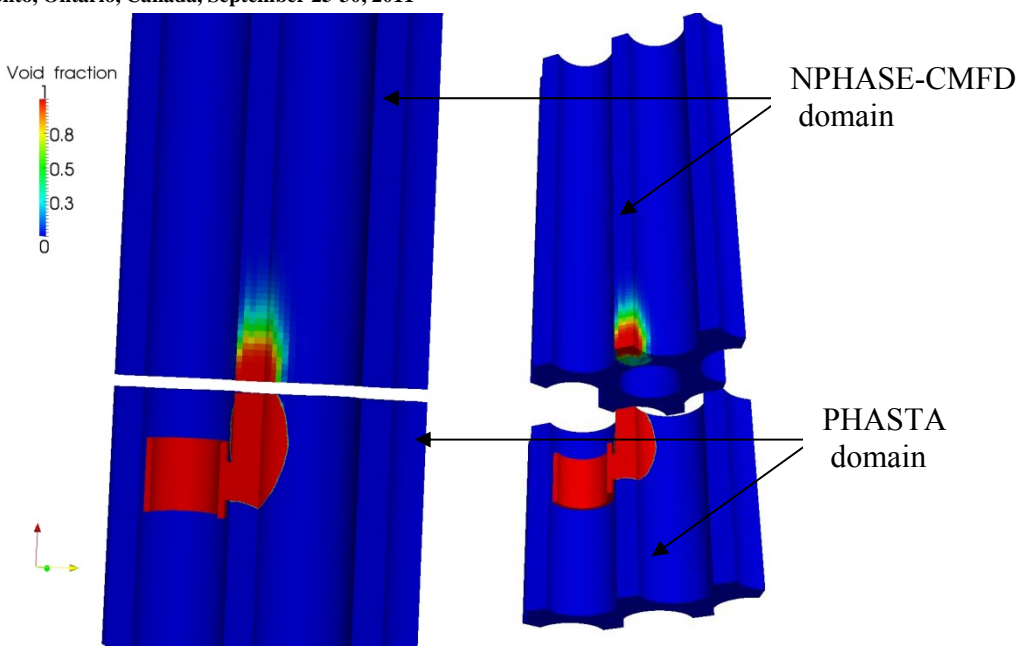


Figure 6. PHASTA/NPHASE-CMFD data transfer: PHASTA domain (bottom part) computes gas (red) and liquid (blue) phase distributions which are averaged to provide the time-varying inflow to NPHASE domain (the average void fraction distribution is also shown).

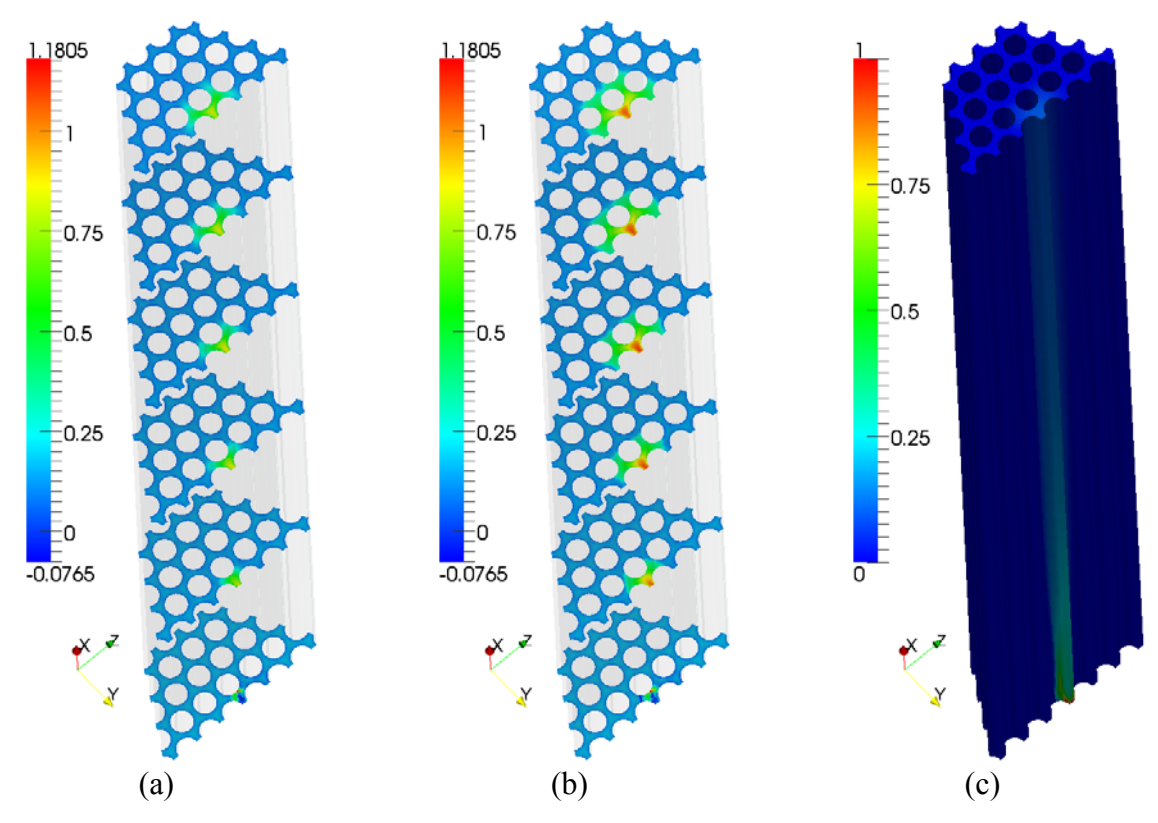


Figure 7. (a) The results of NPHASE-CMFD calculations: (a) axial velocity of the liquid phase; (b) axial velocity component of the gas phase; (c) void fraction. The cross-sections extend between the inlet at the bottom and the outlet at the top, with equally-spaced intervals in between.

4.2. Turbulent liquid coolant case

To test the effect of flow conditions at the inlet to the partially blocked channels, the liquid coolant velocity was increased to approximately 0.24 m/s to make the flow turbulent. The size of cladding breach was the same as before.

4.2.1 PHASTA Calculations

The mesh used for gas injection into the turbulent liquid coolant should be suitable for both DNS and two-phase flow modeling. To monitor the turbulent fluctuations at the data gathering plane for NPHASE-CFMD, a proper boundary layer mesh was used downstream of that plane, from the inlet face up to the location 7.5mm above the middle of the cladding failure location. The boundary layer mesh has 15 elements and the total element size is around 17.5 million. The cross section of the mesh is shown in Figure 8.

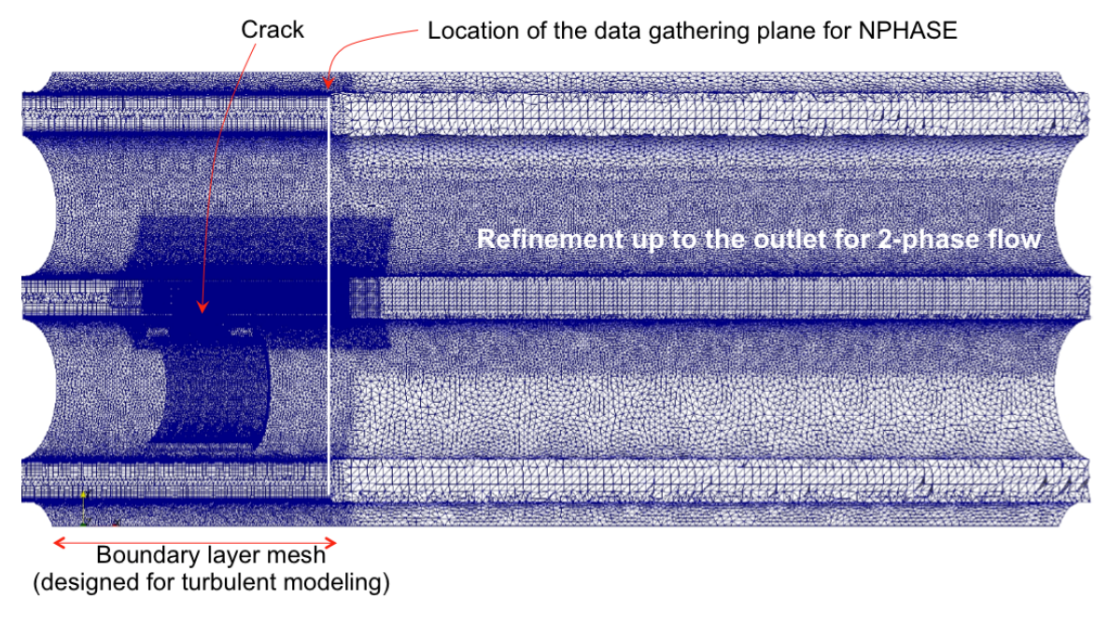


Figure 8. The side view of the mesh used for turbulent liquid simulation. The liquid inlet is on the left and the PHASTA outlet is on the right.

To generate a physically meaningful turbulent flow, a single-phase case with periodic boundary conditions was run first until a fully converged and developed turbulent flow was observed. For the mean velocity of 0.236 *m/s*, the maximum velocity was around 0.33 *m/s*. Three velocity components were recorded at the inlet plane for a full cycle and then post-processed to become usable for PHASTA as inlet boundary conditions. Then, the recorded unsteady turbulent fluctuations were read and introduced into the domain as the inflow. The case was initially run without gas injection, to let the turbulent flow fill the domain and reach the NPHASE-CMFD data-gathering plane. The turbulent flow velocity field right before the start of the injection is shown in Figure 9. The generation of the turbulent inflow field was necessary since the resolved turbulent structures influence the fission gas jet propagation and bubble formation dynamics. Once this complex physical process is fully resolved, the average quantities can be used in the RANS model downstream of the failure.

After initiating turbulent liquid flow conditions inside the domain, the gas injection was started. The gas volume flow rate was the same as in the laminar coolant flow case. Figure 12 shows the PHASTA results at three different physical times. The higher liquid coolant

velocity pushes the gas plume upward faster. It also can be observed that the instability at the interfaces starts sooner when the liquid velocity is higher.

4.2.2 NPHASE-CMFD Calculations

Similarly to the laminar case, the PHASTA data has been collected and transferred to the NPHASE-CMFD code in the turbulent coolant flow regime. As expected, the fast coolant flow influenced the NPHASE results. This is shown in Figure 11. The higher coolant flow rate results in larger local coolant velocities (see Figure 12) and quicker predicted fission gas propagation downstream of the failure zone.

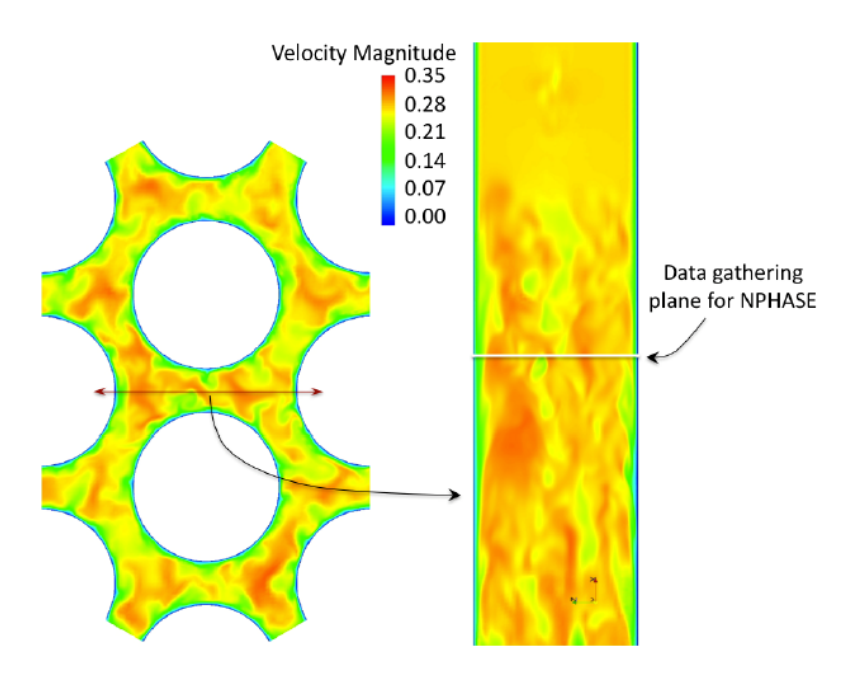


Figure 9. Developed turbulent liquid coolant as the inlet boundary condition (left). The cross section of the domain at the location indicated with the brown arrow on the left figure (right). The bottom part of the right figure is the time varying turbulent inlet BC and the top region has not been filled with the turbulent flow.

5 CONCLUSIONS

A new approach has been presented to multiscale multiphase simulations of reactor transients and accidents. The direct numerical simulation (DNS) and Reynolds Averaged Navier-Stokes (RANS) methods have been applied to different parts of the problem, using the PHASTA and NPHASE-CMFD codes, respectively. An appropriate coupling at the interface between these two solvers has been developed to allow for an interactive interaction between the different-scale solution methods.

It has been demonstrated that the proposed methodology can be used to analyze the consequences of hypothetical local channel blockage accidents in the Gen-IV sodium fast reactor.

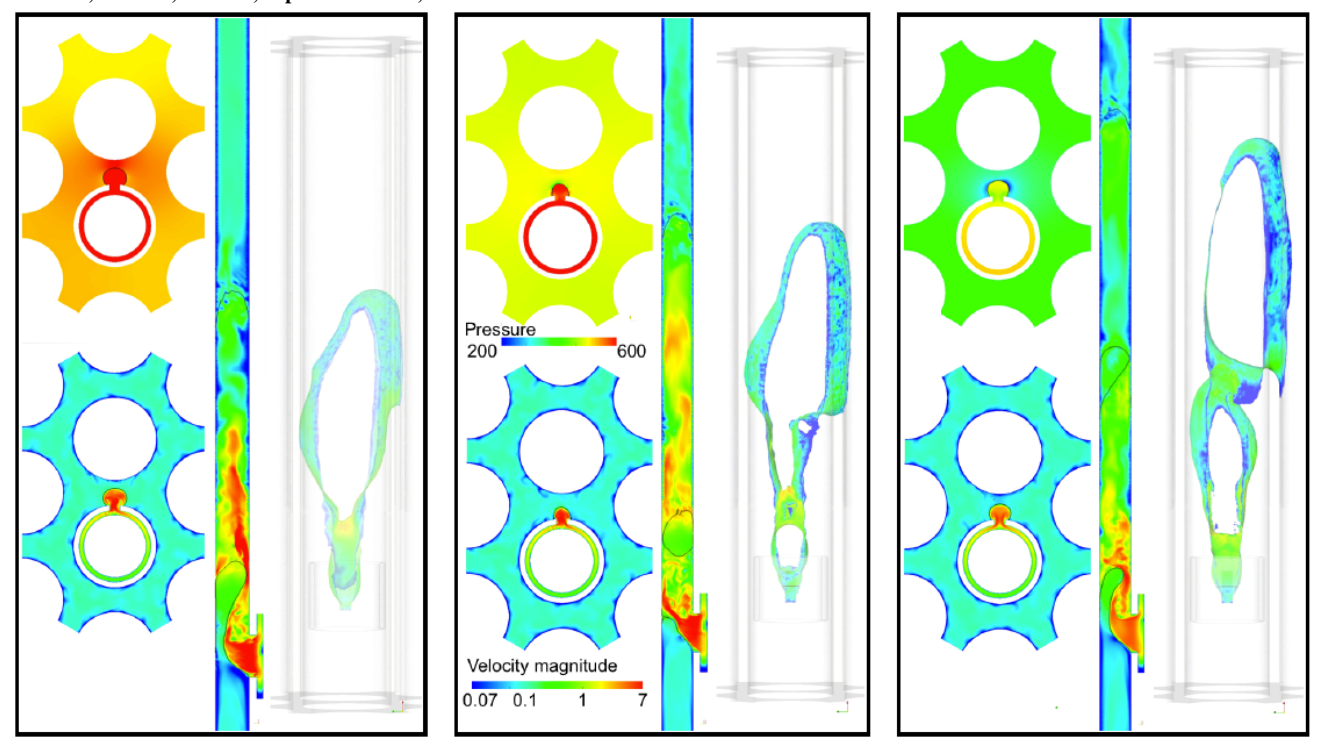


Figure 10. Physical times of 0.08, 0.13 and 0.18 second (up to time step 41000) Each set has two top-views of pressure and velocity fields (Left), one side view of the velocity field (Middle) and a 3D shape of the interface colored by velocity (Right).

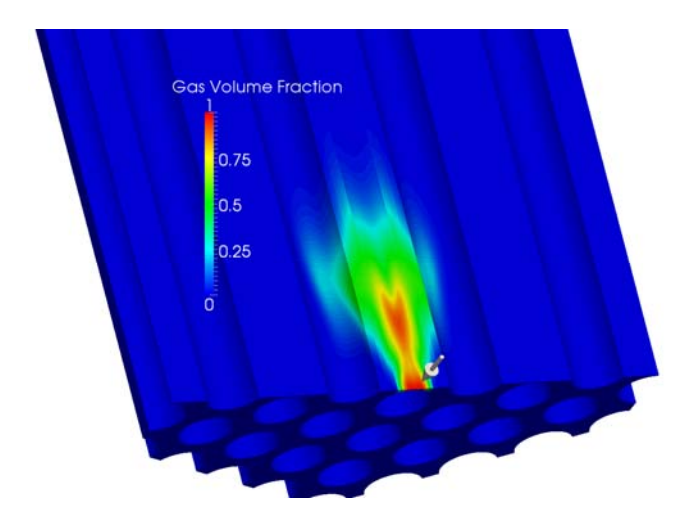


Figure 11. Gas phase volume fraction calculated by NPHASE-CMFD for turbulent liquid flow conditions. The arrow indicates the orientation of the gas discharge into the coolant channel.

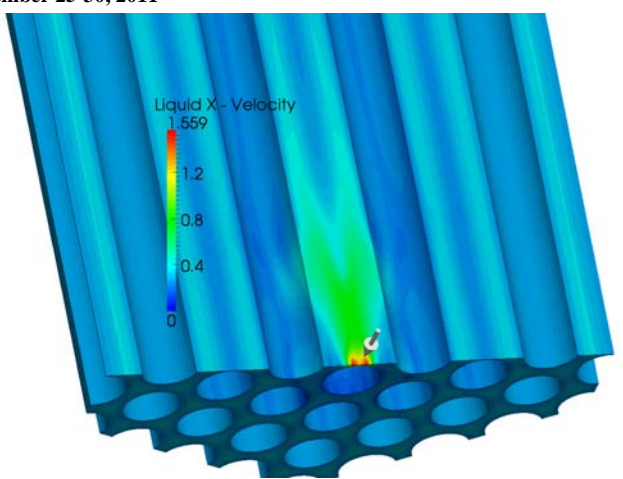


Figure 12. Stream-wise liquid velocity distribution predicted by NPHASE-CMFD.

Acknowledgements

The authors would like to acknowledge the financial support provided to this study by the U.S. Department of Energy and the computation resources provided by the Scientific Computational Research Center (SCOREC) and Computational Center for Nanotechnology Innovations (CCNI) at Rensselaer Polytechnic Institute (RPI).

References

- [1] Antal, S., Ettorre, S., Kunz, R. and Podowski, M., "Development of a next generation computer code for the prediction of multicomponent multiphase flows," Proceeding of the International Meeting on Trends in Numerical and Physical Modeling for Industrial Multiphase Flow, Cargese, France (2000).
- [2] Behafarid, F., Bolotnov, I.A., Podowski, M.Z. and Jansen K.E., "Two phase cross jet in a fuel rod assembly using DNS/Level-Set method", 7th International Conference on Multiphase Flow (ICMF-2010), Tampa, FL, May 30 June 4 (2010).
- [3] Bolotnov, I.A., Antal, S.P., Jansen K.E. and Podowski, M.Z., "Multidimensional Analysis of Fission Gas Discharge following Fuel Element Failure in Sodium Fast Reactor", *The 13th International Topical Meeting on Nuclear Reactor Thermal Hydraulics (NURETH-13)*, Kanazawa City, Japan, September 27 October 2 (2009).
- [4] Bolotnov, I.A., Behafarid, F., Shaver, D., Antal, S.P., Jansen, K.E., Samulyak, R., Wang, S., Wei, H., Podowski, M.Z., "Interaction of Computational Tools for Multiscale Multiphysics Simulation of Generation-IV Reactors", *2010 International Congress on Advances in Nuclear Power Plants (ICAPP'10)*, San Diego, CA, June 13 17 (2010a).
- [5] Bolotnov, I.A., Behafarid, F., Shaver, D., Antal, S.P., Jansen, K.E., Samulyak, R., Wei, H., Podowski, M.Z., "Multiscale Computer Simulation of Fission Gas Discharge during Loss-of-Flow Accident in Sodium Fast Reactor", *Experimental Validation and Application of CFD and CMFD Codes to Nuclear Reactor Safety Issues (CFD4NRS-3)*, Washington D.C., USA, September, 14–16 (2010b).
- [6] Bolotnov, I.A., Jansen, K.E., Drew, D.A., Oberai, A.A., Lahey, R.T., Jr. and Podowski, M.Z., "Detached Direct Numerical Simulation of Turbulent Two-phase

- Bubbly Channel Flow", *Int. J. Multiphase Flow* (2011), doi:10.1016/j.ijmultiphaseflow.2011.03.002
- [7] Gallaway, T., Antal, S.P. and Podowski, M.Z., "Multidimensional Model of Fluid Flow and Heat Transfer in Generation-IV Supercritical Water Reactors", *Nuclear Engineering and Design*, **238**, 1909–1916 (2008).
- [8] Jansen, K. E., Whiting, C.H. and Hulbert, G.M., "A generalized-alpha method for integrating the filtered Navier-Stokes equations with a stabilized finite element method", *Computer Methods in Applied Mechanics and Engineering*, **190**, 3-4, 305-319 (2000).
- [9] Nagrath S., Jansen K. E., Lahey R. T., "Computation of incompressible bubble dynamics with a stabilized finite element level set method", *Computer Methods in Applied Mechanics and Engineering*, **194**, 4565–4587 (2005).
- [10] Sahni, O., Mueller, J., Jansen, K.E., Shephard, M.S. and Taylor, C.A., "Efficient Anisotropic Adaptive Discretization of the Cardiovascular System", *Computer Methods in Applied Mechanics and Engineering*, **195**, 41-43, 5634-5655 (2006).
- [11] Sethian, J. A., "Level Set Methods and Fast Marching Methods", Cambridge University Press. (1999).
- [12] Tejada-Martinez, A.E. and Jansen, K.E., "A parameter- free dynamic subgrid-scale model for large-eddy simulation", *Computer Methods in Applied Mechanics and Engineering*, **194**, No. 9, 1225-1248 (2005).
- [13] Tiwari, P., Antal, S.P. and Podowski, M.Z., "Modeling Shear-induced Diffusion Force in Particulate Flows", *Computers & Fluids*, **38**, 727–737 (2009).
- [14] Tiwari, P., Antal, S.P. and Podowski, M.Z., "Three-Dimensional Fluid Mechanics of Particulate Two-Phase Flows in U-bend and Helical Conduits", *Physics of Fluids*, **18**, 4, 1-18 (2006).
- [15] Tselishcheva, E.A., Antal, S.P. and Podowski, M.Z., "Mechanistic Multidimensional Analysis of Horizontal Two-phase Flows", *Nuclear Engineering and Design* **240**, 405–415 (2010).
- [16] Whiting, C.H. and Jansen, K.E., "A Stabilized Finite Element Formulation For The Incompressible Navier-Stokes Equations Using A Hierarchical Basis," *International Journal of Numerical Methods in Fluids*, **35**, 93-116 (2001).
- [17] Wierzbicki, B.W., Antal, S.P. and Podowski, M.Z., "On the Modeling of Gas Bubble Evolution and Transport using Coupled Level-Set/CFD Method", *Nuclear Technology*, **158**, 2, 261-274 (2007).